



Slow molecular mobility in the crystalline and amorphous solid states of glucose as studied by thermally stimulated depolarization currents (TSDC)

Hermínio P. Diogo^a, Joaquim J. Moura Ramos^{b,*}

^a Centro de Química Estrutural, Complexo I, IST, Universidade Técnica de Lisboa, Av. Rovisco Pais, 1049-001 Lisboa, Portugal

^b CQFM—Centro de Química-Física Molecular and IN—Institute of Nanoscience and Nanotechnology, Instituto Superior Técnico, Universidade Técnica de Lisboa, 1049-001 Lisboa, Portugal

ARTICLE INFO

Article history:

Received 27 March 2008

Received in revised form 25 June 2008

Accepted 1 July 2008

Available online 9 July 2008

Keywords:

α -Relaxation

β -Relaxation

Secondary relaxations

Aging

Fragility

Glass-forming liquids

ABSTRACT

Thermally Stimulated Depolarization Currents (TSDC) measurements on α -D-glucose have been carried out in the temperature region from -165°C (108 K) to 120°C (393 K). The slow molecular mobility was characterized in the crystalline and in the glassy states, as well as in the glass transition region. The influence of aging on the measured TSDC peaks of the secondary relaxation has been discussed and it was concluded that there are motional modes that are aging independent while others are affected by aging. Important discrepancies were reported in the value of the steepness index or fragility (T_g —normalized temperature dependence of the relaxation time) obtained by different, and well-established, experimental techniques. A careful discussion of the possible origins of these discrepancies is presented.

© 2008 Elsevier Ltd. All rights reserved.

1. Introduction

Carbohydrate glasses are thought to play a protective role in the dormant states of desiccation-resistant organisms. Simple saccharides in the amorphous solid state are believed to protect biomacromolecules and cells during freezing, dehydration, and storage.^{1,2} Different hypotheses for this ability have been formulated, but the problem is not yet elucidated. The mechanism by which these sugars help to protect the integrity of biomacromolecules seems to be a consequence of two factors: (a) specific hydrogen-bonding interactions between the sugar and the macromolecule outer surface which helps to maintain the three-dimensional structure of the protein³ and (b) tendency to provide a viscous glassy state, allowing to a non-specific restriction of conformational flexibility of the macromolecule.⁴ In this context, the study of the evolution of the molecular mobility from high temperature down to the glassy state is a relevant aspect to the understanding of the biopreservation ability. On the other hand, amorphous carbohydrates are important substances in the industrial area. In particular, they are often used in pharmaceutical, cosmetic, and food industries to effectively encapsulate, stabilize, and ultimately control the release of labile active materials.^{5,6} Furthermore, carbohydrates exhibit advantageous properties: they are readily available with high purity and

low toxicity, they are good glass-formers with generally high glass transition temperatures (T_g). This set of properties makes them adequate materials to store pharmaceutical and food products at room temperature and allow them to be shipped without cooling, avoiding the inconvenience of dry ice packing. Despite the frequent use of sugars as protecting agents, little is known about molecular mobility in glassy sugars.

Recent studies of molecular dynamics of amorphous carbohydrates using the Thermally Stimulated Depolarization Currents (TSDC) relaxation technique complement those previously published using other relaxation techniques such as NMR^{7–9} and dielectric relaxation spectroscopy (DRS).^{10–12} These TSDC studies show several features in common with glass-forming materials in general, but showed also some intriguing results concerning the glass transition in some disaccharides as trehalose, cellobiose and gentiobiose,¹³ and also in salicin.¹⁴ Furthermore, it has been recently shown, on the basis of TSDC data, that different types of secondary relaxations are differently influenced by aging.^{13,15,16} In fact, as will be discussed later, part of the secondary mobility appears as aging independent, while another part is clearly affected by aging. These findings will give an interesting contribution to the emergence of a fully coherent view of the molecular origin of the secondary relaxations, namely of the Johari–Goldstein relaxation. In the case of sugar melts, both pyranose/furanose and α/β equilibria exist, and this isomerization complicates the interpretation of the relaxation behaviour.^{17,10,18} The pyranose/furanose

* Corresponding author. Fax: +351 21 8464455.

E-mail address: mouramos@ist.utl.pt (J. J. Moura Ramos).

isomerization is likely to have a stronger effect in the dielectric experiments given that it implies a more extensive structural rearrangement. For D-glucose, only pyranose forms are reported, in opposition to D-fructose where a large amount of furanose forms (up to 46%) can exist in the melt depending on the thermal history.¹⁷ The equilibrium between the two anomers α and β in melted glucose occurs at a ratio α/β of 0.8 according to some authors,¹⁹ and of 1.0 according to others.¹⁷ The equilibration time in the melt is relatively fast: 15 min at one degree above the melting temperature.^{19,20}

The observation of a diversity of relaxation behaviour in carbohydrates may have implications for their ability to protect biological molecules and structures against the stresses induced by freezing and drying. It is commonly considered that the main structural or α -relaxation is coupled with deteriorative processes. Below T_g , however, some kind of motions give rise to the secondary relaxations and it may be that some of these motions are coupled to the protective and chemical stabilization activity of carbohydrates during freezing, drying, and storage. In the present paper, we use the Thermally Stimulated Depolarization Currents (TSDC) relaxation technique to study the molecular mobility of α -D-glucose in the crystalline state, and of glucose in the amorphous solid state (obtained by cooling the equilibrated melt). Our results will be discussed and compared with those obtained by other experimental techniques.

2. Experimental

2.1. Materials

α -D-Glucose was purchased from Acros (purity 99+%) and used as received. The melting peak of our samples, obtained by DSC, showed an onset at $T_{on} = 159.5^\circ\text{C}$ and a maximum at $T_{max} = 162.0^\circ\text{C}$ (heating rate $10^\circ\text{C min}^{-1}$). The values $T_{on} = 158.29 \pm 0.106^\circ\text{C}$ (DSC, $10^\circ\text{C min}^{-1}$),²¹ $T_{on} = 143^\circ\text{C}$ and $T_{max} = 158^\circ\text{C}$ (DSC, 5°C min^{-1})²² and $T_{max} = 143^\circ\text{C}$ (DSC, 5°C min^{-1})²³ were previously reported in the literature. The melting enthalpy, also obtained by DSC, was $\Delta_{fus}H = (34.8 \pm 0.2) \text{ kJ mol}^{-1}$ (mean over six determinations; the reported uncertainty corresponds to the standard deviation of the mean). The values previously reported in the literature are $\Delta_{fus}H = 32.3 \text{ kJ mol}^{-1}$ obtained by DSC²² and $\Delta_{fus}H = 31.4 \text{ kJ mol}^{-1}$ obtained using a 'radiation' calorimeter.²⁴

2.2. Thermally stimulated depolarization currents

Thermally Stimulated Depolarization Current (TSDC) experiments were carried out with a TSC/RMA spectrometer (TherMold, Stamford, CT, USA) covering the range from -170 to $+400^\circ\text{C}$. For TSDC measurements, the sample was placed between the electrodes of a parallel plane capacitor and immersed in an atmosphere of high purity helium (1.1 bar). The TSDC technique is adequate to probe slow molecular motions (20–3000 s). The fact that the relaxation time of the motional processes is temperature dependent, and becomes longer as temperature decreases, allows to make it exceedingly long (frozen process) compared with the timescale of the experiment. In order to analyse specific regions of the TSDC spectrum the partial polarization (PP) procedure, also called thermal windowing or cleaning or sampling, is often used. This PP method, where the polarizing field is applied in a narrow temperature interval, allows decomposing a complex distributed relaxation into its single motional modes. In the limit of a very narrow polarization window, the retained polarization (and of course the current peak, that is, the result of a partial polarization (PP) experiment) would correspond to a single, individual dipolar motion.^{25,26} The physical background of the TSDC technique is

presented elsewhere.^{27,28} The basic description of the TSDC experiment, and the discussion of the nature of the information it provides, is presented in detail in recent publications.^{25,26,29,30}

2.3. Differential scanning calorimetry (DSC)

The calorimetric measurements were performed with a 2920 MDSC system from TA Instruments Inc. Dry high purity He gas with a flow rate of $30 \text{ cm}^3/\text{min}$ was purged through the sample. Cooling was accomplished with the liquid nitrogen cooling accessory (LNCA) which provides automatic and continuous programmed sample cooling down to -150°C . The samples of ~ 8 – 15 mg were introduced in aluminium pans, hermetically sealed using a sample encapsulating press. An empty aluminium pan, identical to that used for the sample, was used as the reference. The baseline was calibrated scanning the temperature domain of the experiments with an empty pan. The temperature scale of the instrument had been previously calibrated by taking the onsets of the fusion peaks of the five standards (*n*-decane, *n*-octadecane, hexatriacontane, indium, and tin). The calibration of the heat flow scale was checked by measuring the enthalpy of fusion of indium.³¹ More calibration details are given elsewhere.³²

3. Results and discussion

The slow molecular mobility of glucose will be characterized using the following methodology: (i) the partial polarization (PP) procedure is used to get the dielectric manifestation of narrowly distributed motional modes, that is the partial polarization peaks; (ii) the PP peaks are analyzed (using the so-called Bucci method³³) in order to obtain the temperature dependent relaxation time, $\tau(T)$, of each motional mode; (iii) fitting each $\tau(T)$ line to an appropriate kinetic equation (Arrhenius, Eyring, Vogel, etc.) provides the kinetic parameters which characterize the different motional modes (activation energy and prefactor, activation enthalpy and entropy, etc.). An usual representation of the kinetic data is a graph of the activation energy (or enthalpy) of the motional modes as a function of the corresponding temperature location (temperature of maximum intensity of the PP peak, T_{max}). This is the so-called Starkweather plot where it is useful to include a reference line, the so-called Starkweather line,^{34,35} or zero entropy line, that depicts the behaviour of non-cooperative relaxations. As will be seen later, the Starkweather plot is a useful way of presenting TSDC data in order to highlight the degree of cooperativity of the different motional processes.

3.1. Mobility in the amorphous state

Glucose in the solid amorphous phase was prepared by melting the crystal of α -D-glucose at 170°C and cooling the isotropic liquid (recall that the melting peak observed in DSC shows a maximum $T_{max} = 162.0^\circ\text{C}$ for a heating rate of $10^\circ\text{C min}^{-1}$). The samples must be carefully heated around their melting temperature since it is easily caramelized at higher temperature. The substance displayed excellent glass-forming ability, with a wide supercooled liquid temperature region and high thermal stability against crystallization. The calorimetric glass transition temperature of our samples, considered as the onset of the glass transition signal, was $T_g = 34.4 \pm 0.3^\circ\text{C}$ (average of five determinations at $10^\circ\text{C min}^{-1}$, where the uncertainty indicated corresponds to the standard deviation of the mean), which can be compared with the values $T_g = 34.77 \pm 1.38^\circ\text{C}$ ²¹ and $T_g = 36^\circ\text{C}$ ³⁶ previously reported. Our TSDC results discussed later showed a glass transition global peak with maximum intensity at $T_{max} = 35.9^\circ\text{C}$ (at 8°C min^{-1}). Furthermore, the most intense partial polarization mode of the glass

transition distribution shows maximum intensity at $T_{\max} = 30.3^\circ\text{C}$ (at 4°C min^{-1}). Those temperatures are in good agreement with the calorimetric results. Let us also consider the value $T_g = 27^\circ\text{C}$ obtained from the temperature dependence of the band position of the OH stretching.^{37,38} Finally, the heat capacity jump in the glass transformation range was found to be $\Delta C_p = (0.74 \pm 0.02) \text{ J } ^\circ\text{C}^{-1} \text{ g}^{-1} = (133.7 \pm 2.9) \text{ J } ^\circ\text{C}^{-1} \text{ mol}^{-1}$ (average over 12 experiments, the uncertainty indicated is the standard deviation of the mean), in reasonable agreement with the values $\Delta C_p = 0.77 \pm 0.02 \text{ J } ^\circ\text{C}^{-1} \text{ g}^{-1}$,²¹ $\Delta C_p = 0.79 \text{ J } ^\circ\text{C}^{-1} \text{ g}^{-1}$ ³⁶ and $\Delta C_p = 0.63 \text{ J } ^\circ\text{C}^{-1} \text{ g}^{-1}$ ²² previously reported.

3.1.1. Secondary relaxations

The sub- T_g mobility, and particularly the so-called β -relaxation (Johari–Goldstein)³⁹ is a residual mobility in the glassy state that is believed to be important in achieving stability, and thus constitutes a crucial issue from the point of view of biopreservation. The TSDC results we obtained below the glass transition temperature show that the sub- T_g mobility in amorphous glucose appears in the TSDC spectrum in a wide temperature region from -165°C (the lower temperature available to our equipment) to the glass transformation range. Note that in the crystalline α -D-glucose, no signal of mobility was observed in this temperature range. Figure 1 shows the results of several partial polarization experiments carried out in the temperature region of the secondary relaxation. It reveals a clear structure of the relaxation peaks, consequence of a hierarchy of the molecular motions. In fact, three different groups of motional modes can be considered from the observation of Figure 1, named a, b, and c in the order of increasing temperature. In the lower temperature side, the motional modes of group a show dielectric strengths that decrease with increasing temperature. In the temperature region between -70°C and -40°C another group of motional modes are observed (group b) and, finally, above -35°C (group c) show dielectric strengths that strongly increase with increasing temperature.

The activation energy was found to be distributed between 30 and 65 kJ mol^{-1} , in agreement with the value of the Arrhenius activation energy 42 kJ mol^{-1} obtained by Dielectric Relaxation Spectroscopy¹⁰ and 59 kJ mol^{-1} determined by DSC.⁴⁰ Furthermore, the pre-exponential factors are of the order of the Debye time 10^{-13} s or, stated differently, the motional components of this mobility have negligible activation entropy. It is worth to recall

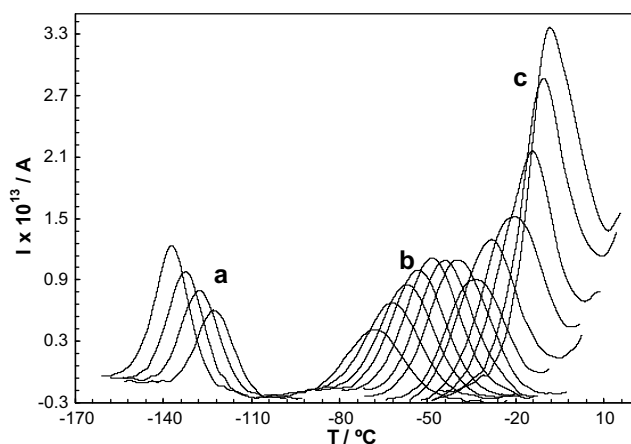


Figure 1. Partial polarization components of the sub- T_g molecular mobility of amorphous glucose. The polarization temperatures, T_p , were from -140 to -125°C and from -70 to -10°C , with intervals of 5°C . The other relevant experimental conditions were strength of the polarizing electric field, $E = 450 \text{ V mm}^{-1}$; polarization time, $t_p = 5 \text{ min}$; width of the polarization window, $\Delta T = 2^\circ\text{C}$; heating rate, $r = 4^\circ\text{C min}^{-1}$.

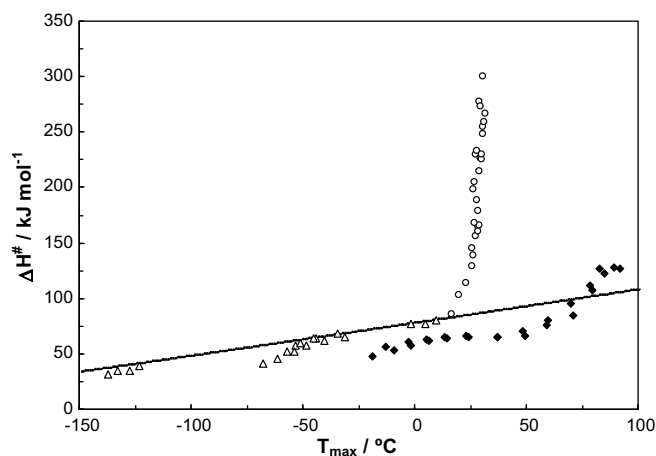


Figure 2. Activation enthalpy, ΔH^\ddagger , of a series of motional modes of the crystalline α -D-glucose (filled lozenges) and of the amorphous solid glucose (open triangles and circles), as a function of the peak's location, T_m . The line is the zero entropy line.

that the quantity $\tau_D = \frac{h}{kT_0} = 1.76 \times 10^{-13} \text{ s}$ (with $T_0 = 273.15 \text{ K}$), often called Debye time, represents the characteristic time, at room temperature, of a process with no activation Gibbs energy. It is the pre-exponential factor of the Eyring equation, so that the deviation of the Arrhenius prefactor, τ_0 , from τ_D correlates to the activation entropy associated with reorientation in the relaxation process.⁴¹ High values of the activation entropy, or smaller value of τ_0 relative to τ_D , can be interpreted to arise from cooperativity of the orientational motion. Figure 2 shows the so-called Starkweather plot³⁵ in which the line is the zero entropy line. The open triangles correspond to motional processes of groups a, b, and c in Figure 1. They show negligible activation entropies and can thus be considered as modes of motion of the secondary relaxations. The motional modes corresponding to group c are motions that are activated at temperatures close to the glass transformation range and appear as a pre-peak in the lower temperature vicinity of the α -peak (see below).

The secondary relaxation of amorphous glucose is thus broad and distributed in energy, composed by a complex mixture of motional modes, all of them local, low amplitude, and non-cooperative. The origin of this distribution is ascribed to a variety of microenvironments that exist in the solid glassy state, but the identification of the molecular motions associated with those processes is still a matter of debate. According to some authors^{42,43} the secondary relaxation in glucose arises from motions of the exocyclic hydroxymethyl, CH_2OH , groups rather from intermolecular degrees of freedom. An opposite scenario^{39,44} envisages the β -relaxation as a molecular reorientation which occurs in high free volume and high entropy regions immersed in an otherwise rigid glass matrix. It is to be noted in this context that an important ^{13}C NMR study with specifically labelled anhydrous glucose⁹ concluded that the mobility of the glucose ring and of the exocyclic hydroxymethyl group are strongly correlated so that the mobility of the CH_2OH group alone should not be used to explain the β -relaxation process.

3.1.2. Effect of aging on the secondary relaxations

Considering the complexity of the secondary relaxations present in amorphous glucose, we decided to focus a particular attention on the influence of aging on its different segments. Figure 3 shows the results of four global experiments (wide polarization window) that were designed to this purpose.

Lines 1 and 2 concern the amorphous unaged sample, while lines 3 and 4 concern the amorphous glucose aged during 48 h at 21°C . The difference between the results 1 and 3 on the one hand,

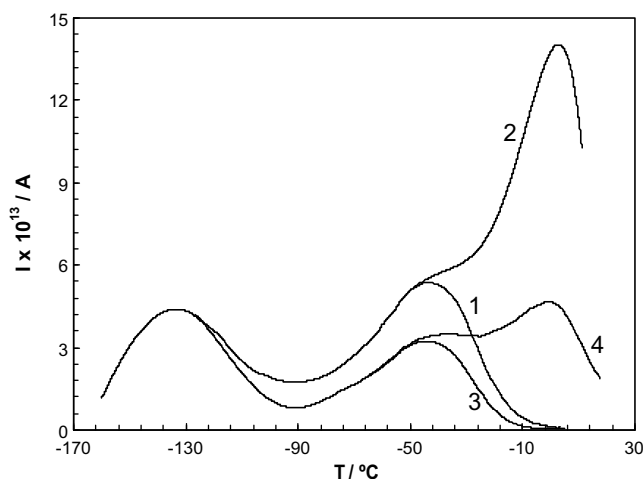


Figure 3. TSDC thermogram showing the secondary relaxations of amorphous unaged (curves 1 and 2) and aged (curves 3 and 4) glucose. The relevant experimental parameters were strength of the polarizing electric field, $E = 450 \text{ V mm}^{-1}$, polarization time, $t_p = 5 \text{ min}$, freezing temperature, $T_0 = -165^\circ\text{C}$, heating rate, $r = 8^\circ\text{C min}^{-1}$. The polarization temperature was $T_p = -40^\circ\text{C}$ (curves 1 and 3) and $T_p = -5^\circ\text{C}$ (curves 2 and 4). The aged sample was annealed prior to the experiment at the aging temperature of $T_a = 21^\circ\text{C}$ during a period of time of 48 h.

and 2 and 4 on the other, is that experiments 1 and 3 were designed in order to activate the motional modes of the groups a and b in Figure 1 (the polarization temperature of the experiments is $T_p = -40^\circ\text{C}$), while in experiments 2 and 4 the motional modes of group c (Fig. 1) are also activated (the polarization temperature of the experiments is $T_p = -5^\circ\text{C}$).

Let us recall that this secondary relaxation is a feature of the amorphous state given that it is absent in the crystalline form of glucose. The results displayed in Figure 3 show that the lower temperature modes of the secondary relaxation, we call fast β -relaxation (group a in Fig. 1), are not influenced by aging, but that the higher temperature components (groups b and c in Fig. 1) are strongly affected. Furthermore, those manifestations of the physical aging on the secondary relaxations are reversible as the aging effects can be erased by heating above T_g to the metastable liquid state.

Given that density increases, and the free volume decreases, on structural relaxation, it was suggested that the faster motional modes (detected at lower temperatures), not affected by aging, must have an intramolecular origin.^{13,15,16} These are local motions that consist of internal rotations of one part of a molecule relative to the other part, or conformational modifications of a cyclic unit, which occur without significant interference of the neighbouring molecules. In the case of glucose, these local motions could be associated to the pendant hydroxymethyl group,^{10,42} probably correlated with the mobility of the glucose ring.⁹ On the other hand, the slower motional modes, affected by aging, have probably an intermolecular origin and, in the case of glucose, they seem to correspond to two different kinds of molecular motions (modes belonging to group b and to group c in Fig. 1). Let us emphasize that the depolarization peaks of group c in Fig. 1 (as well as those of groups a and b) correspond indeed to mobility components of the secondary relaxation of glucose: first of all because the polarization temperature of those partial polarization peaks is less than -5°C , much lower in comparison with the glass transition temperature of glucose which is $T_g = 35^\circ\text{C}$; second because from the observation of Figure 2 it becomes clear that the secondary relaxation (the motional modes with negligible activation entropy) extends at least to temperatures up to $\sim 15^\circ\text{C}$. We are thus in the presence of two aging dependent mobility modes that constitute the so-called slow β or Johari–Goldstein relaxation.³⁹

3.1.3. Glass transition relaxation and fragility

Figure 4 presents the results of a series of partial polarization experiments carried out in the temperature region of the glass transformation.

An important feature of the motional processes associated with the glass transition relaxation is, as noted before, the so-called deviation from the zero entropy behaviour,³⁵ that is illustrated in Figure 2. The open circles on the right-hand side, that correspond to the motional modes in the temperature region of the glass transformation (some of them corresponding to the peaks in Fig. 4), show a strong departure from the line which describes the behaviour of local and non-cooperative relaxations. This indicates the cooperative nature of the molecular mobility that is released on heating through the glass transformation range.

The peak with higher intensity in Figure 4, was obtained with a polarization temperature $T_p = 26^\circ\text{C}$, and is the manifestation of a mobility component that is characteristic of the glass transition of glucose. It shows a maximum intensity at $T_M = 30.3^\circ\text{C}$ (at 4°C min^{-1}) which is identified with the glass transition temperature provided by TSDC. The analysis of this singular peak allows the determination of the activation energy for the structural relaxation, and also of the fragility index of the glass-forming system.²⁵ The relaxation time at T_M was found to be $\tau(T_M) = (45.1 \pm 0.6) \text{ s}$ and the activation energy of the structural relaxation $E_a(T_M) = (245.9 \pm 4.4) \text{ kJ mol}^{-1}$ (both values are a mean over fifteen determinations, and the reported uncertainty corresponds to the standard deviation of the mean).

The fragility of a glass-forming liquid refers to the loss of the short range order with increasing temperature across the glass transition, and is defined as the T_g -normalized temperature dependence of the structural relaxation times:⁴⁵

$$m = \left[\frac{d \log_{10} \tau(T)}{d(T_g/T)} \right]_{T=T_g} = \frac{1}{2.303} \left[\frac{E_a(T_g)}{RT_g} \right] \quad (1)$$

In this definition, $E_a(T_g)$ is the apparent activation energy in the equilibrium state (i.e., in the supercooled liquid) at (or just above) T_g . The fragility values of glucose published in literature are very scattered: $m = 31$ ³⁶ and $m = 70$ ²¹ from DSC data, $m = 54$,¹⁰ $m = 52$,¹¹ $m = 87$,⁴³ $m = 96$,¹² and $m = 101$ ⁴⁴ from Dielectric Relaxa-

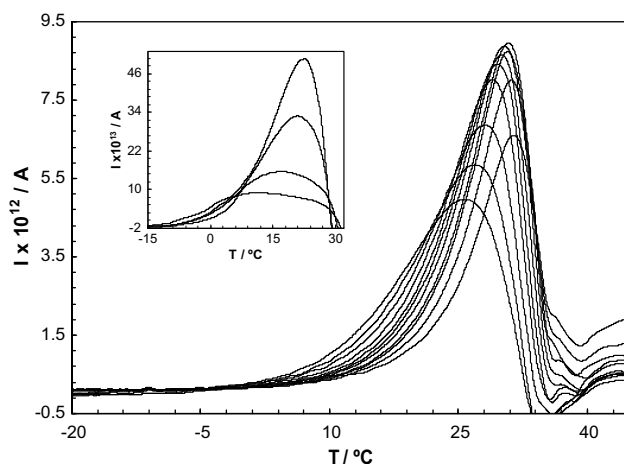


Figure 4. Partial polarization (PP) components of the glass transition relaxation of glucose. The polarization temperatures, T_p , were from 16 to 22°C with intervals of 2°C and from 23 to 29°C with intervals of 1°C . The sequence of the peaks is such that T_{max} increases as T_p increases. The other experimental conditions were strength of the polarizing electric field, $E = 450 \text{ V mm}^{-1}$; polarization time, $t_p = 5 \text{ min}$; width of the polarization window, $\Delta T = 2 \text{ K}$; heating rate, $r = 4 \text{ K min}^{-1}$. The inset shows the peaks corresponding to the lower temperature partial polarization modes of the glass transition distribution, obtained with polarization temperatures $T_p = 0, 5, 10$, and 12°C .

tion Spectroscopy (DRS) data, and $m = 105$ calculated by Angell et al.⁴⁶ from previously published viscosity data.⁴⁷ From our TSDC data we obtain⁴⁸ $m = 43 \pm 1$ (mean over 15 determinations; the reported uncertainty corresponds to the standard deviation of the mean), indicating that glucose is a relatively strong glass-forming liquid, with a TSDC fragility slightly lower than that of glycerol.⁴⁹

A significant scatter of the fragility values obtained from different experimental techniques is sometimes observed. In the case of indomethacin, values near $m = 60$ are obtained by TSDC⁵⁰ and by DSC,³¹ while $m = 81$ is obtained from dielectric relaxation data.⁵¹ Discrepancies of the same order of magnitude have also been reported in the case of sorbitol and fructose.⁵² However, the discrepancy is much more striking in the case of 4,4'-methylenebis(*N,N*-diglycidylaniline) (MBDA), a highly functionalized epoxide. The steepness index or fragility, m , of MBDA was determined by three different and independent procedures based on TSDC data, leading to values in very good mutual agreement: $m \cong 47$.⁵³ However, the value obtained from the heating rate dependence of the onset temperature of the DSC signal gives $m = 78$,⁵³ whereas the value based on dielectric relaxation data is $m = 102$.⁵⁴ The strong differences in the fragility values obtained using different experimental techniques (namely DSC, DRS, and TSDC) and different methodologies based on the same technique, is a troubling problem that needs to be looked straightforward in order to understand the origin.

It is to be noted that the determinations by dielectric relaxation spectroscopy often imply important temperature extrapolations, which can introduce significant uncertainties, all the more since the molecular mobility in the temperature domain of the glass transformation clearly displays a non-Arrhenius behaviour. In the case of TSDC, the influence of aging effects taking place during heating scans performed at relatively low rates should also be considered. An important difference between the two dielectric techniques TSDC and DRS is that TSDC looks at the glass transition from the lower temperature side (no polarization can be retained above T_g), while DRS analyses the glass transition using data obtained at temperatures higher than T_g (supercooled liquid). As a consequence, physical aging can interfere in an undesirable way in the case of TSDC results, in temperature regions that include the glass transformation region (and temperatures not far below). This interference should be particularly important in the case of very fragile systems and for heating scans performed at relatively low rates. However, the results of experiments carried out at different heating rates in MBDA⁵³ as well as in indomethacin⁵⁰ seem to discard this suspicion. The contamination by aging can also occur in DSC results for the same reasons invoked in the case of TSDC. Furthermore, it was very clearly demonstrated⁵² that the shape of the DSC signature of the glass transition is very sensitive to the whole thermal history of the sample, that is, on the previous cooling rate and on temperature and time of residence below T_g . In fact, it was found that the heating rate effect on the different points of the heat capacity jump (on the characteristic temperatures as the onset, endset, and midpoint temperatures) is significantly different, leading to different values of the activation energy of the structural relaxation, and consequently of the fragility index. Finally, we must realize that the temperature dependence of the enthalpic relaxation can be different from that of dielectric relaxation. In order to understand the scattering of the fragility values we need to study several highly complex and fragile glass-forming systems by independent techniques, and try to find some correlation between the molecular structure, the liquid complexity and the observed differences.

It is well known that the fragility values obtained by TSDC, $m(\text{tsdc})$, are in general lower than those obtained by DRS, $m(\text{drs})$, and that the difference between those values tends to be higher for fragile glass formers.⁴⁹ In order to understand these differences we need to recall that TSDC looks at the glass transition from the

Table 1

Values of the TSDC fragility, $m(\text{tsdc})$, of the DRS fragility, $m(\text{drs})$, of the ratio $m(\text{drs})/m(\text{tsdc})$, and of the experimental non-linearity parameter, x_{exp}

	$m(\text{tsdc})$	$m(\text{drs})$	selected $m(\text{drs})$	$m(\text{tsdc})/m(\text{drs})$	x_{exp}
Fructose	34	92; ¹² 53 ¹⁰	70	0.49	0.755 ²¹
Glucose	43	96; ¹² 87; ⁴⁴ 58 ¹⁰	87	0.49	0.497 ²¹
PET	81 ⁵⁸	166; ^{58,61} 156 ⁶²	160	0.51	0.49 ⁵⁸

lower temperature side (from the glassy state), in opposition to Dielectric Relaxation Spectroscopy that mainly uses data obtained at temperatures higher than T_g .⁴⁹ An essential feature of the glass transition relaxation behaviour is *non-linearity*, which accounts for the effect of the structure of the glass on the relaxation time.^{55–57} The equation of Tool–Narayanaswamy–Moynihan (TNM), a generalized form of the Arrhenius equation:

$$\tau = \tau_0 \exp \left(\frac{x\Delta h^*}{RT} + \frac{(1-x)\Delta h^*}{RT_f} \right) \quad (2)$$

where τ_0 , x ($0 \leq x \leq 1$) and Δh^* are constants, arises from a model that aims to describe the non-linearity. The constant x is the so-called non-linearity parameter which specifies the structure of the glass, and Δh^* is the activation energy at T_g of the equilibrium melt. Cooling below T_g freezes the equilibrium melt into a constant structure glass (characterized by the fictive temperature, T_f), so that the temperature dependence of the relaxation time arises solely from the first term in Eq. 2. As a consequence, and according to the TNM model, the slope of the Arrhenius plot at $T_g/T = 1$ will change from Δh^* at higher temperatures (equilibrium melt) to $x\Delta h^*$ at lower temperatures (constant structure glass). This is the so-called 'return to Arrhenius', such that the temperature independent product $x\Delta h^*$ corresponds to the activation energy of the motions in the frozen, non-annealed glass, which can be, in this context, identified with $E_a(T_M)$, the activation energy determined by TSDC.^{58–60} This idea appears as a reasonable hypotheses that explains, at least in some cases, the discrepancies between the fragility values obtained by TSDC, $m(\text{tsdc})$, and by DRS, $m(\text{drs})$. A very small value of the x parameter indicates an extremely non-linear relaxation. The experimental determination of the non-linearity parameter exists only for a small number of glass-forming systems, and comparison of the values of the ratio $m(\text{tsdc})/m(\text{drs})$ with those of x is made in Table 1.

Despite the scattering of the fragility values obtained from dielectric relaxation spectroscopy by different authors, it is clear from Table 1 that $m(\text{tsdc})$ is smaller than $m(\text{drs})$. Furthermore, the fact that the values of the ratio $m(\text{tsdc})/m(\text{drs})$ compare well with those of the experimental x indicate that it is reasonable to consider the fragility index determined by TSDC as a characteristic of the glassy state at the temperature of the boundary with the glass transformation range.

3.2. Mobility in the crystalline state

In the crystalline phase, a slow molecular mobility was detected by TSDC. Figure 5 shows some partial polarization peaks of this mobility. The very high reproducibility of the experimental results leads us to believe that this relaxation peak originates from dipolar reorientation motions rather than from material discontinuities (Maxwell–Wagner effects).

The temperature dependent relaxation time of the PP peaks of this mobility was obtained by the usual Bucci method,³³ and the results indicate that we are dealing with localized molecular motions. In fact, the activation enthalpy of the different motional modes of crystalline glucose, represented in Figure 2 as a function of the temperature location of the corresponding peak (full

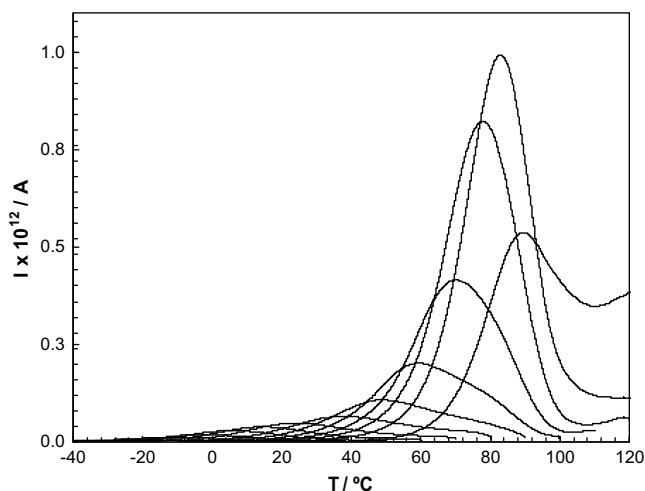


Figure 5. Partial polarization (PP) components of the relaxation in the crystalline phase of glucose. The polarization temperatures, T_p , were from -60 to 90 °C, with intervals of 10 °C. The sequence of the peaks is such that T_{max} increases as T_p increases. The other experimental conditions were strength of the polarizing electric field, $E = 450$ V mm $^{-1}$; polarization time, $t_p = 5$ min; width of the polarization window, $\Delta T = 2$ °C; heating rate, $r = 4$ °C min $^{-1}$.

lozenges), show small deviations from the Starkweather line.³⁵ Note also from Figures 2 and 5 that the molecular mobility in crystalline glucose is thermally activated at very low temperatures compared with the melting temperature ($T_{fus} = 160$ °C). Furthermore, we conclude from Figure 5 that the lower temperature motional modes of this relaxation (that broadly extend from -30 up to 50 °C) show a low-dielectric strength, while the higher modes involve the reorientation of a bigger quantity of dipole moment. We are aware that the attribution of this mobility at the molecular level is not easy. On the other hand, the TSDC studies of mobility in organic low molecular weight dielectrics are relatively scarce.⁶³ However, it seems reasonable to accept that the weakening of the hydrogen bonds that occurs with increasing temperature is at the origin of a smooth mobility, local in nature, and characterized by low amplitude and low-dielectric strength. On the other hand, further heating causes stronger weakening of the hydrogen bonds and expansion of the dimensions of the unit cell, which allows a further release of molecular mobility, with higher amplitude but always local in nature, given that no modification of the crystal structure is observed in this temperature region. The wide temperature interval of this mobility in crystalline glucose seems to be a feature of this particular substance when compared with other crystals like pentitols⁶⁴ and salicylsalicylic acid⁶⁵ where the mobility in the crystal appears in a narrower temperature interval.

4. Conclusions

The study by TSDC of the molecular mobility in the crystalline α -D-glucose showed a well-defined and broad relaxation (activated between -40 and 90 °C) that corresponds to localized or non-cooperative motions.

The mobility in the amorphous solid prepared from the crystalline α -D-glucose showed a broad and complex secondary relaxation revealing a clear structure with three kinds of molecular motions, and with activation energies distributed between 30 and 65 kJ mol $^{-1}$. It was found that the lower temperature components of this complex secondary mobility are aging independent, while the higher temperature components are affected by aging. On the other hand, the analysis of the structural or main relaxation

indicated that the activation energy at the glass transition temperature ($T_g = 30$ °C at 4 °C min $^{-1}$) is $E_a(T_g) = 246$ kJ mol $^{-1}$, so that the fragility index is $m = 43$. This value indicates that glucose is a relatively strong glass-forming liquid. Attention is drawn to the scattering of the fragility values provided by different experimental techniques and from different methodologies based on the same technique. A brief discussion of the possible origins of these discrepancies is presented.

The understanding of the slow molecular mobility in the amorphous solid state is important on different grounds, including nucleation and crystallization processes, preservation of biomacromolecules, cells and tissues, and storage of pharmaceutical and food products. The evidence for the interdependence between the molecular mobility and the chemical stability of amorphous materials enhanced the motivation for an active research in this area. In this context, the technique of Thermally Stimulated Currents appears as a very useful technique helping the clarification of the nature of the secondary relaxations and providing specific information on the α -relaxation. The present work on glucose illustrates the usefulness of the technique and characterises the specific features of the mobility of this carbohydrate.

References

1. Crowe, J. H.; Carpenter, J. F.; Crowe, L. M. *Ann. Rev. Physiol.* **1998**, *60*, 73–103.
2. Buitink, J.; Leprince, O. *Cryobiology* **2004**, *48*, 215–228.
3. Carpenter, J. F.; Crowe, J. H. *Cryobiology* **1988**, *25*, 459–470.
4. Green, J. L.; Angell, C. A. *J. Phys. Chem.* **1989**, *93*, 2880–2882.
5. Yu, L. *Adv. Drug Delivery Rev.* **2001**, *48*, 27–42.
6. Gunning, Y. M.; Gunning, P. A.; Kemsley, E. K.; Parker, R.; Ring, S. G.; Wilson, R. H.; Blake, A. J. *Agric. Food Chem.* **1999**, *47*, 5198–5205.
7. Hills, B. P.; Pardoe, K. J. *Mol. Liq.* **1995**, *63*, 229–237.
8. Hills, B. P.; Wang, Y. L.; Tang, H.-R. *Mol. Phys.* **2001**, *99*, 1679–1687.
9. van Dusschoten, D.; Tracht, U.; Heuer, A.; Spiess, H. W. *J. Phys. Chem. A* **1999**, *103*, 8359–8364.
10. Noel, T. R.; Parker, R.; Ring, S. G. *Carbohydr. Res.* **2000**, *329*, 839–845.
11. Noel, T. R.; Ring, S. G.; Whittam, M. A. *J. Phys. Chem.* **1992**, *96*, 5662–5667.
12. Kaminski, K.; Kaminska, E.; Paluch, M.; Ziolo, J.; Ngai, K. L. *J. Phys. Chem. B* **2006**, *110*, 25045–25049.
13. Moura Ramos, J. J.; Pinto, S. S.; Diogo, H. P. *ChemPhysChem* **2007**, *8*, 2391–2396.
14. Diogo, H. P.; Pinto, S. S.; Moura Ramos, J. J. *Int. J. Pharm.* **2008**, *358*, 192–197.
15. Moura Ramos, J. J.; Diogo, H. P.; Pinto, S. S. *J. Chem. Phys.* **2007**, *126*, 144506/1–6.
16. Moura Ramos, J. J.; Diogo, H. P.; Pinto, S. S. *Thermochim. Acta* **2008**, *467*, 107–112.
17. Fan, J.; Angell, C. A. *Thermochim. Acta* **1995**, *266*, 9–30.
18. Tombari, E.; Cardelli, C.; Salvetti, G.; Johari, G. P. *J. Mol. Struct.* **2001**, *559*, 245–254.
19. Broido, A.; Houminer, Y.; Patai, S. J. *Chem. Soc. B* **1996**, 411–414.
20. Pincock, R. E.; Kiovsky, T. E. *J. Chem. Soc., Chem. Commun.* **1966**, 864–866.
21. Wungtanagorn, R.; Schmidt, S. J. *Thermochim. Acta* **2001**, *369*, 95–116.
22. Roos, Y. *Carbohydr. Res.* **1993**, *238*, 39–48.
23. Hatakeyama, T.; Yoshida, H.; Nagasaki, C.; Hatakeyama, H. *Polymer* **1976**, *17*, 559–562.
24. Parks, G. S.; Thomas, S. B. *J. Am. Chem. Soc.* **1934**, *56*, 1423.
25. Correia, N. T.; Moura Ramos, J. J.; Descamps, M.; Collins, G. *Pharm. Res.* **2001**, *18*, 1767–1774.
26. Correia, N. T.; Alvarez, C.; Moura Ramos, J. J.; Descamps, M. *J. Phys. Chem. B* **2001**, *105*, 5663–5669.
27. Chen, R.; Kirsch, Y. *Analysis of Thermally Stimulated Processes*; Pergamon Press: Oxford, 1981.
28. van Turnhout, J. *Thermally Stimulated Discharge of Polymer Electrets*; Elsevier Sci.: Amsterdam, 1975.
29. Teyssedre, G.; Mezghani, S.; Bernes, A.; Lacabanne, C. Thermally Stimulated Currents of Polymers. In *Dielectric Spectroscopy of Polymeric Materials*; Runt, J. P., Fitzgerald, J. J., Eds.; American Chemical Society: Washington, 1997.
30. Sauer, B. B. Thermally Stimulated Currents: Recent Developments in Characterisation and Analysis of Polymers. In *Handbook of Thermal Analysis and Calorimetry*; Gallager, P. K., Ed.; Applications to Polymers and Plastics; Cheng, S. Z. D. Ed.; Elsevier: Amsterdam, 2002; pp 653–711.
31. Moura Ramos, J. J.; Taveira-Marques, R.; Diogo, H. P. *J. Pharm. Sci.* **2004**, *93*, 1503–1507.
32. Moura Ramos, J.; Afonso, C.; Branco, L. J. *Therm. Anal. Calorim.* **2003**, *71*, 659–666.
33. Bucci, C.; Fieschi, R.; Guidi, G. *Phys. Rev.* **1966**, *148*, 816–823.
34. Starkweather, H. W. *Macromolecules* **1981**, *14*, 1277–1281.
35. Sauer, B. B.; Avakian, P.; Starkweather, H. W.; Hsiao, B. S. *Macromolecules* **1990**, *23*, 5119–5126.
36. Kawai, K.; Hagiwara, T.; Takai, R.; Suzuki, T. *Pharm. Res.* **2005**, *22*, 490–495.

37. Wolkers, W. F.; Oldenhof, H.; Alberda, M.; Hoekstra, F. A. *Biochim. Biophys. Acta* **1998**, 1379, 83–96.
38. Wolkers, W. F.; Oliver, A. E.; Tablin, F.; Crowe, J. H. *Carbohydr. Res.* **2004**, 339, 1077–1085.
39. Johari, G. P.; Goldstein, M. J. *Chem. Phys.* **1970**, 53, 2372–2388.
40. Vyazovkin, S.; Dranca, I. *Pharm. Res.* **2006**, 23, 2158–2164.
41. Rachocki, A.; Markiewicz, E.; Tritt-Goc, J. *Acta Phys. Pol., A* **2005**, 108, 137–145.
42. Noel, T. R.; Parker, R.; Ring, S. G. *Carbohydr. Res.* **1996**, 282, 193–206.
43. Gangasharan; Murthy, S. S. N. *J. Phys. Chem.* **1995**, 99, 12349–12354.
44. Chan, R. K.; Pathmanathan, K.; Johari, G. P. *J. Phys. Chem.* **1986**, 90, 6358–6362.
45. Bohmer, R.; Angell, C. A. Local and Global Relaxations in Glass-Forming Materials. In *Disorder Effects on Relaxational Processes*; Richert, R., Blumen, A., Eds.; Springer: Berlin, 1994; pp 11–54.
46. Angell, C. A.; Bressel, R. D.; Green, J. L.; Kanno, H.; Oguni, M.; Sare, E. J. *J. Food Eng.* **1994**, 22, 115–142.
47. Ollett, A. L.; Parker, R. J. *Text. Stud.* **1990**, 21, 355–362.
48. Moura Ramos, J. J.; Correia, N. T. *Phys. Chem. Chem. Phys.* **2001**, 3, 5575–5578.
49. Moura Ramos, J. J.; Correia, N. T.; Diogo, H. P. *J. Non-Cryst. Solids* **2006**, 352, 4753–4757.
50. Moura Ramos, J. J.; Correia, N. T.; Taveira-Marques, R.; Collins, G. *Pharm. Res.* **2002**, 19, 1879–1884.
51. He, R.; Craig, D. Q. M. *J. Pharm. Pharmacol.* **2001**, 53, 41–48.
52. Simatos, D.; Blond, G.; Roudaut, G.; Champion, D.; Perez, J.; Faivre, A. L. *J. Therm. Anal.* **1996**, 47, 1419–1436.
53. Diogo, H. P.; Moura Ramos, J. J. *J. Mol. Liq.* **2006**, 129, 138–146.
54. Casalini, R.; Paluch, M.; Psurek, T.; Roland, C. M. *J. Mol. Liq.* **2004**, 111, 53–60.
55. Hodge, I. M. *J. Non-Cryst. Solids* **1994**, 169, 211–266.
56. Hutchinson, J. M. *Progr. Polym. Sci.* **1995**, 20, 703–760.
57. Borde, B.; Bizot, H.; Vigier, G.; Buleon, A. *Carbohydr. Polym.* **2002**, 48, 83–96.
58. Saiter, J. M.; Dargent, E.; Kattan, M.; Cabot, C.; Grenet, J. *Polymer* **2003**, 44, 3995–4001.
59. Hutchinson, J. M. *Polym. Int.* **1998**, 47, 56–64.
60. Dargent, E.; Bureau, E.; Delbreilh, L.; Zmailan, A.; Saiter, J. M. *Polymer* **2005**, 46, 3090–3095.
61. Saiter, A.; Hess, M.; Saiter, J. M.; Grenet, J. *Macromol. Symp.* **2001**, 174, 165–173.
62. Qin, Q.; McKenna, G. B. *J. Non-Cryst. Solids* **2006**, 352, 2977–2985.
63. Gun'ko, V. M.; Zarko, V. I.; Goncharuk, E. V.; Andriyko, L. S.; Turov, V. V.; Nychiporuk, Y. M.; Lebeda, R.; Skubiszewska-Zieba, J.; Gabchak, A. L.; Osovskii, V. D.; Ptushinskii, Y. G.; Yurchenko, G. R.; Mishchuk, O. A.; Gorbik, P. P.; Pissis, P.; Blitz, J. P. *Adv. Colloid Interface Sci.* **2007**, 131, 1–89.
64. Diogo, H. P.; Pinto, S. S.; Moura Ramos, J. J. *Carbohydr. Res.* **2007**, 342, 961–969.
65. Moura Ramos, J. J.; Correia, N. T.; Diogo, H. P.; Alvarez, C.; Ezquerro, T. A. *J. Non-Cryst. Solids* **2005**, 351, 3600–3606.